LARGE-EDDY SIMULATION OF THE THREE-DIMENSIONAL UNSTABLE FLOW IN A LID-RIVEN CAVITY

Elie Luis M. Padilla
Federal University of Uberlândia
epadilla@mecanica.ufu.br

André Leibsohn Martins
CENPES - Petrobras
aleibsohn@petrobras.com.br

Aristeu Silveira-Neto
Federal University of Uberlândia
aristeus@mecanica.ufu.br

Abstract. *Transitional and turbulent flows in a three-dimensional lid-driven cavity has been performed employing a large–eddy simulation methodology with dynamical and Smagorinsky subgrid-scale modes. The volume method in cartesian coordinates is applied on staggered girds, considering second order temporal and spatial schemes. The tree-dimensional structures as spanwise inward and outward currents, the end-wall corner vortices and the Taylor-Gortler-like vortices were observed. As Reynolds number is increased the instabilities appear in the lower part of the cavity and, for the high Reynolds number the unstable flow becomes fully turbulent. The Taylor-Gortler-like vortices were distorted due to onset of turbulence regime. The qualitative and quantitative results showed a good agreement with experimental and numerical dates of other authors, also, the comparative analyze between the sub-grid scale models is presented.*

Keywords*: Unstable flow, lid-driven cavity, large-eddy simulation.*

1. Introduction

The lid-driven cavity flows have several important technological applications in different areas of engineering, moreover treated of flows with high complexity that until the present time is investigations reasons. The simplicity of the geometry that delimits the problem contrasts with the diversity of structures that if form and according to literature, this characteristic it became in a classic problem to test numerical models

The representation of cavities of square section with infinite axial length, bidimensional cavities, is has been widely studied and is now a standard case test for new computational schemes. Benjamin and Denny (1979), Ghia et al. (1982) e Botella e Peyret (1998) they are some of the many existing works, of which Ghia et al. (1982) is frequent referenced. Ghia et al. employed finite-difference method with stream function-vorticity formulation, using uniform cartesian grids.

Due the difficulty of to study three-dimensional lid-driven cavity, only in 80s the pioneering experimental work of koseff and Street (1984) allowed show that cavity flows were three-dimensional in nature. Moreover were observed pattern characteristics as primary and secondary eddies and structures as the end-wall corner vortices, the spanwise inward and outward currents and the Taylor-Gortler-like vortices. Recently Migeon et al. (2003) considered time three-dimensional development inside standard parallelepiped lid-driven cavities at Reynolds number 1000; the results show the formation and development of vorticals structures and initial phase of the Taylor-Gortler-like vortices development.

The recent progress in numerical analysis and computer hardware has made it possible to adequate three-dimensional analyze. Ku et al. (1987) and Babu and Korpela (1994) through of solving of the three-dimensional Navier-Stokes equations, had presented comparisons between bi and three-dimensional results for cubic cavity. On the other hand, Iwatsu et al. (1989) show the flow topology from projection of the streamlines on planes for several Reynolds number and Sheu and Tsai (2002) carry through the same for Reynolds number 400. Unstable laminar flows that show the existence of Taylor-Gortler-like, has were computed by Iwatsu et al. (1990), Zang et al. (1994) and Chiang et al. (1996). The turbulent flows has been simulated using direct numerical simulation methodology by Leriche and Gavvirakis (2000) and large-eddy simulation by Zang et al. (1993), Deshpande and Milton (1998), Hassan Barsamian (2001). These works compared the results with experimental dates of koseff and Street (1984) and show turbulent statistical characteristics and instantaneous behavior.

2. Problem Formulation and Turbulent Model

The geometry of problem is depicted in Fig. 1, it is treated of a lid-driven cubical cavity of side $L = 1\ m$. The lid surface moves in the positive x direction with velocity $U = 1.0\ m/s$. The normal walls to direction x are called of downstream and upstream walls, the normal wall direction y is called bottom wall and the normal walls to direction z are called side walls.

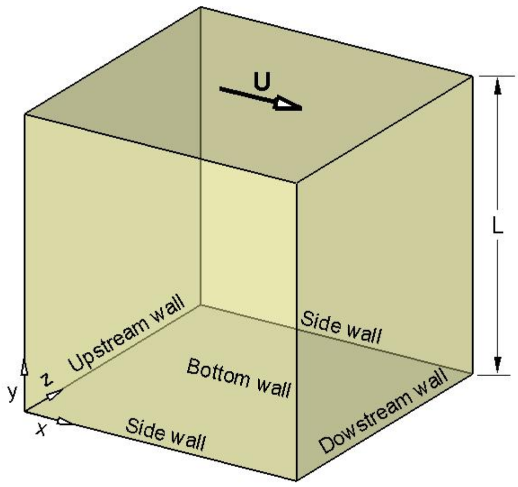

Figure 1. Lid-driven cubical cavity geometry.

The fluid confined is isothermal and incompressible, with constant proprieties. The computational modeling requires solving three-dimensional flows equations, or either solving the Navier-Stokes equations. These equations in dimensional form and cartesian coordinates are as follows:

$$\nabla.\vec{u} = 0\,, \tag{1}$$

$$\frac{\partial \vec{u}}{\partial t} + \nabla.(\vec{u}\vec{u}) = -\frac{1}{\rho}\nabla\vec{p} + \nabla.\left[\nu(\nabla\vec{u} + \nabla\vec{u}^T)\right], \tag{2}$$

where the velocity vector $\vec{u}$ has components u, v, w in x, y, z directions, respectively, p is the pressure field, ρ is the density and ν is the cinematic viscosity. According large-eddy simulation methodology (Smagorinsky, 1963), the filtering process are applied on the governed equations for separate the fields that contains the large and sub-grid scales. This filtering process gives rise to the generalized sub-grid scale Reynolds stress, defined as $\tau_{ij} = -(\overline{u_i u_j} - \bar{u}_i \bar{u}_j)$, as described by Silveira-Neto et al. (2002). The tensor τ_{ij} is modeled using the Boussinesq hypothesis:

$$\tau_{ij} = -\nu_t 2\bar{S}_{ij} + \frac{2}{3}k\delta_{ij}\,, \tag{3}$$

where ν_t is the turbulent viscosity, $\bar{S}_{ij} = (1/2)(\partial\bar{u}_i/\partial x_j + \partial\bar{u}_j/\partial x_i)$ is the strain rate of the resolved field and k is the kinetic turbulent energy. Considering the Eqs. (1-3), the filtered Navier-Stokes equations are written as:

$$\nabla.\vec{\bar{u}} = 0\,, \tag{4}$$

$$\frac{\partial \vec{\bar{u}}}{\partial t} + \nabla.(\vec{\bar{u}}\ \vec{\bar{u}}) = -\frac{1}{\rho}\nabla\vec{\bar{p}} + \nabla.\left[(\nu + \nu_t)(\nabla\vec{\bar{u}} + \nabla\vec{\bar{u}}^T)\right]. \tag{5}$$

Two sub-grid scale models were used to approximate the sub-grid scale Reynolds stress, the Smagorinsky and dynamic models. The Smagorinsky model proposed by Smagorinsky (1963), is based on the equilibrium hypothesis, where the production can be equal the dissipation of sub-grid scale turbulent kinetic energy due to the viscosity effects. The form derived is:

$$\nu_t = (C_s\Delta)^2 \,|\,\overline{S}\,|\,, \tag{6}$$

where C_s is Smagorinsky coefficient, Δ is the filter length scale and $|S| = (\overline{S}_{ij}\overline{S}_{ij})^{1/2}$. C_s may take different values in different flows, here were used two values 0.1 (Lilly,) and 0.18 (Gravemeier, 2003). In the dynamic sub-grid scale model proposed by Germano et al. (1991), the parameter model can be computed as function of spatial coordinate and time. This model removes many of the difficulties and deficiencies of Smagorinsky model. According to the expression presented by Germano et al. (1991) and modificated by Lilly (1992):

$$\nu_t = C\Delta^2 \,|\,\overline{S}\,|\,, \tag{7}$$

with the dynamic coefficient C give by:

$$C = -\frac{1}{2}\frac{L_{ij}M_{ij}}{M_{ij}M_{ij}}, \qquad L_{ij} = \widehat{\overline{u}_i\overline{u}_j} - \hat{\overline{u}}_i\hat{\overline{u}}_j\,, \qquad M_{ij} = \hat{\Delta}^2\,|\,\hat{\overline{S}}\,|\,\hat{\overline{S}}_{ij} - \widehat{\Delta^2\,|\,\overline{S}\,|\,\overline{S}_{ij}}\,. \tag{8}$$

where $\hat{\Delta} = 2\Delta$ is the filter test length scale. The influence of the filter test on flow is very important as demostred in Padilla and Silveira-Neto (2003), here used the discreet filter proposed by Padilla (2004).

3. Numerical Method

In order to perform the equations discretization, the finite volume method was employed on staggered grid, having second order schemes in space and time (Piomelli, 2000): central differencing an Adams-Brashforth schemes, respectively. The pressure velocity coupling method was the fractional step (Kim and Moin, 1985), where the steps named predictor and corrector are used. The pressure correction is evaluated by solving the Poisson equation using strongly implicit procedure method, as proposed by Stone (1968).

The time step is evaluated following the CFL stability criteria. Moreover, uniform and non-uniform (concentrated near walls) meshes are employed.

4. Results

The lid-driven square cavity and the lid-driven cubical cavity were considered for the bi and thee-dimensional simulations.

4.1. Bidimentional cavity

The bidimensional configuration was approached considering a minimum of volumes and periodicity boundary condition in the axial direction. Several cases with $Re \leq 1000$ had been considered, of which they are presented resulted for $Re = 100$ and 1000, simulated with uniforms meshes of 40x40x2 and 50x50x2 in the horizontal, vertical and axial directions, respectively.

Figure 1 shows the streamlines displayed on the colored vorticity distribution for Reynolds number 100 and 1000. The standard flow in both cases present the primary vortex and two secondary vortices, with changes of form and size as Re increases. Qualitatively these results are similar to the numerical results of Ghia et al. (1982) and Botella and Peyret (1998). The changes in the flow in function of the increment of Re are reflected in the displacement of vortices centers, that quantified are very approached with the results of the works adobe mentioned and with the ones of Schreiber and Keller (1983) and Goyon (1996).

For bigger comparative details the data of Ghia et al. (1982) are used. The Fig. 2 depicts velocity profiles on the $x = 0.5$ (left) and $y = 0.5$ (right) line for horizontal and vertical velocity, respectively. For low Re are not necessary dense meshes to get good results (as example $Re = 100$), but for $Re = 1000$ a small difference observed between the profiles gotten with meshes 40x40x2 and 50x50x2, as well as the data of Ghia et al. (1982). As Re increases, bigger gradients in the lid-driven and the near walls are formed, as consequence dense meshes or non-uniform meshes are necessary. Of general form, the results have a good agreement with the numerical results of Ghia et al. (1982).

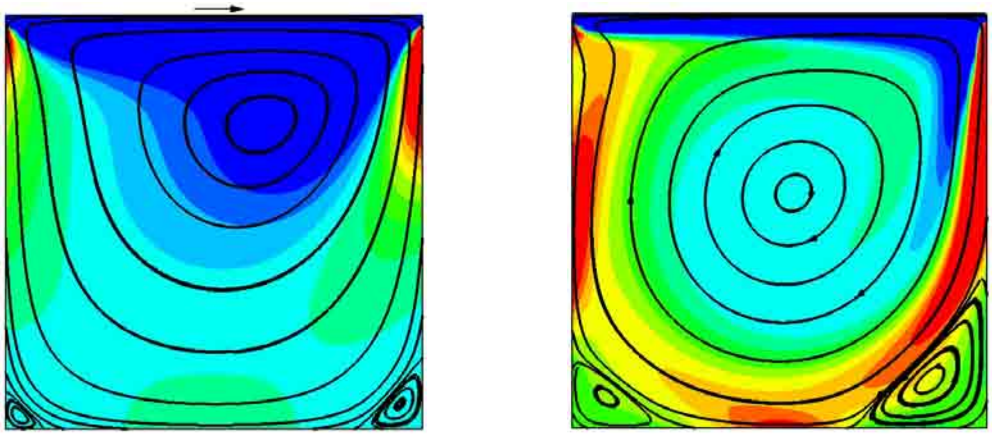

Figure 2. Streamlines on vorticity fields (+: red and -: blue). Left: Re =100; right: Re =1000.

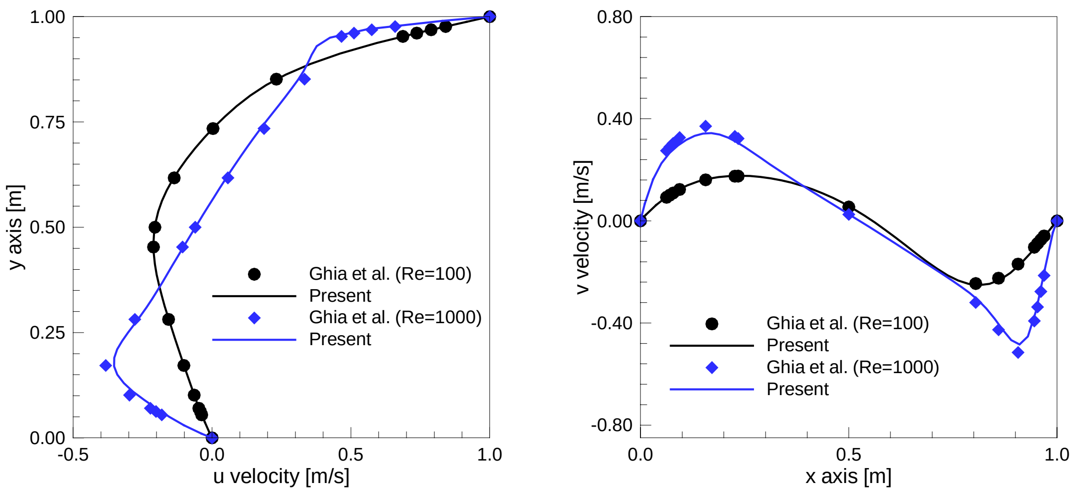

Figure 3. Comparison of profiles at the mid-sectional line. Left: horizontal velocity; right: vertical velocity.

4.2. Three-dimensional cavity

Results for several Reynolds number $Re \leq 10000$, corresponding to the stable and unstable flows, was obtained using uniform and non-uniform meshes. The simulations for $Re \leq 1000$ were performed with both types of meshes and without sub-grid scale model. For $Re \leq 3200$ were performed with uniform meshes and Smagorinsky and dynamic sub-grid scale models.

The important experimental work of Koseff and Street (1982) and Koseff and Street (1984) demonstrated that flows inside lid-driven cavity are three-dimensional in nature, showing that beyond the structures observed in the bidimensional configurations, were formed others: the end-wall corner vortices, the spanwise inward and outward currents and the Taylor-Gortler-like counter-rotating vortices (visualized by Migeon et al. 2003 so). Figure 4 shows the projections of the streamlines on three equidistant planes in z direction (left) and x direction (right) at Re =400, considering an uniform mesh of 50x50x50. The full-developed state it allows to observe that the flow is symmetric on the mid-plane $z = 0.5$. The mid-plane clearly show the primary and secondary vortices and side walls plane show the projections of the end-wall corner vortices. The downstream and upstream walls it allows to evidence the presence of the spanwise outward current inside the downstream and upstream secondary eddies and the mid-plane $x = 0.5$ show the projection of the spanwise outward current inside the primary eddy. The results show the good agreement with the numerical data of Sheu and Tsai (2002).

Evidently the differences with the bidimensional solutions are well known, which are bigger as Re increases, these differences are larger for cubical cavities, however diminish for larger aspect ratio height/axial length, as demonstrated by Chiang et al. (1998).

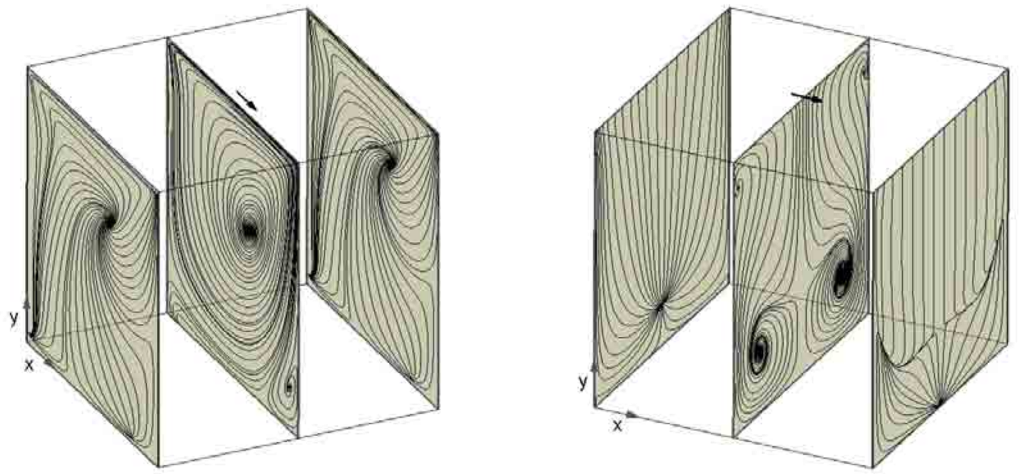

Figure 4. The projections of the streamlines on equidistant planes at Re =400.

Exists discrepancy respect of the Reynolds number from which the flow to pass of steady to unstable. Visualizations of Aidum et al. (1991) to allow conclude that the flow becomes unstable at the approximate Re =825, considering aspect ratio of 3, but the numerical result of Chiang et al. (1998) it reports the value of Re = 1250 (same conditions). Other references consider the value of $Re \approx$ 1000. When the Reynolds number is increased for 3200 the flow is clearly unstable (Fig. 5: left) and when is increased up to Re =10000 the flow show high degree of instability and turbulence (Figs. 5-8).

Figure 5 depicts time distribution of horizontal velocity at three y stations on the x = 0.5, z = 0.5 line and Re = 3200 and 10000, performed with non-uniforms meshes of 40x40x40. It can be seen that the flow starts from rest and becomes quickly unstable, where the fluctuations were maiores near of bottom wall and minors in the center of the cavity. The sign of the signal it is related with the dynamics of the primary eddies, that in the nearness of the lid-driven is positive, it oscillates between positive and negative in the center and negative and in the nearness of the bottom wall is negative. The flow for Re = 1000 shows oscillations of u velocity with larger amplitude and presence of multiple frequencies that form an irregular standard, characteristic standard of the turbulent flows.

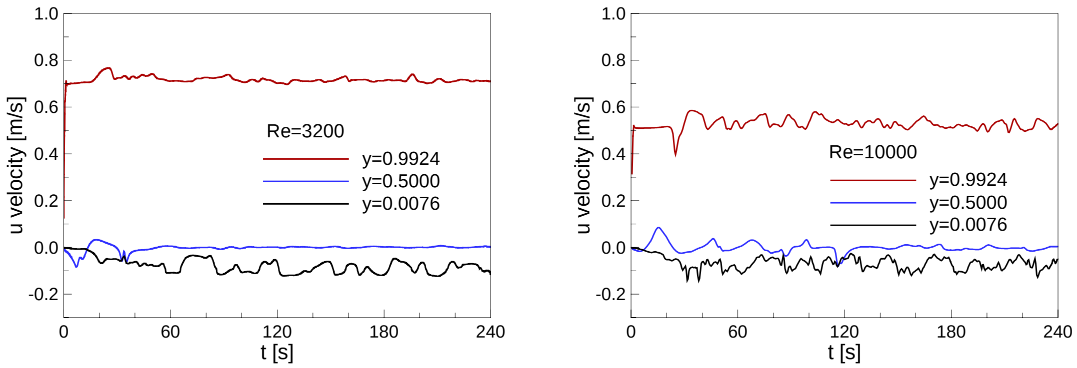

Figure 5. Time distribution of horizontal velocity at various y stations on the $x = 0.5$, $z = 0.5$ line.

According to observations of Koseff and Street (1984) and Prasad and Koseff (1989), the flow for Reynolds numbers below 5000 is essentially laminar and that transition to turbulence regime takes place in the range of 6000-8000. However the large-eddy simulation methodology has been employed for flows of $Re \geq$ 3200.

The results of the flow in lid-driven cavity for Re =10000 were compared with experimental dates of Prasad and Koseff (1989). Comparisons between Smagorinsky and dynamic sub-grid scale models are also carried through. Where the Smagorinsky model considers two values for the Smagorinsky coefficient. The results are presented in statistical quantifications form (mean velocities and root-mean square velocities) and instantaneous vorticity isosurfaces. The statistics of the different fields it considers the last ones 100 s.

Figures 6 and 7 shows comparison of profiles at the mid-sectional plane (z =0.5 m), left side on the x = 0.5 m line and right side on the y = 0.5 m. Mean velocity profiles of horizontal and vertical velocity present good comparison everywhere except near the downstream wall, as seen in Fig. 6. The influence of the use of different values of C_s is notorious, mainly in regions next of lid-driven, downstream and upstream walls, but is not possible to differentiate the advantage of a value on another one, however the Fig. 7 permit one better analysis. On the other hand, for both the components of the velocity, the dynamic sub-grid scale model obtain better agreement with experimental data that the Smagorinsky sub-grid scale model.

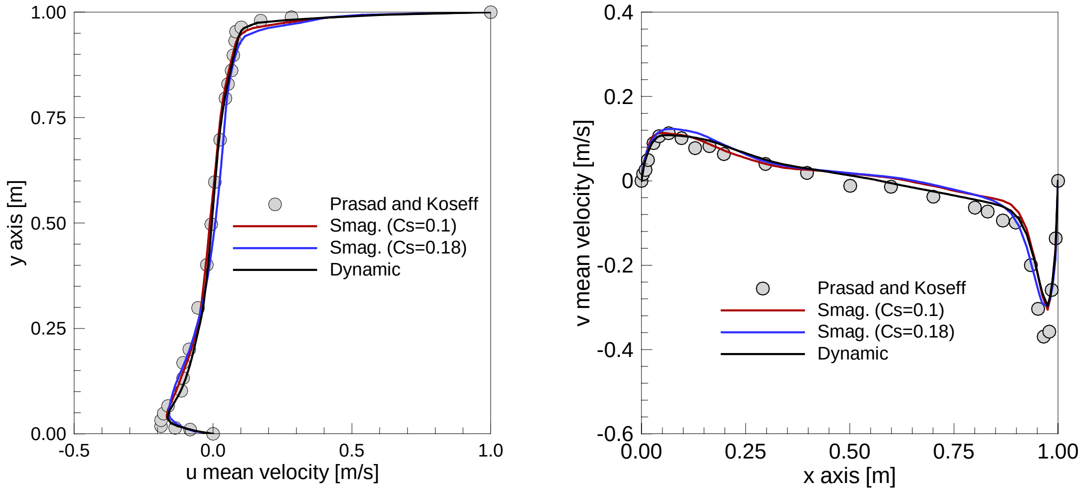

Figure 6. Comparison of the mean velocity at Re =10000. Left: horizontal velocity; right: vertical velocity.

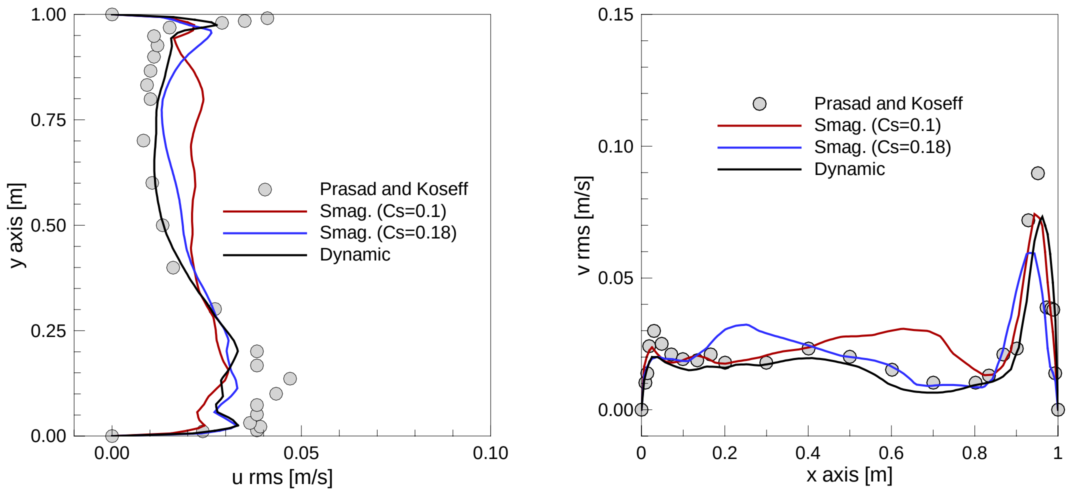

Figure 7. Comparison of the fluctuating velocity at Re =10000. Left: horizontal velocity: right: vertical velocity.

Root-mean square velocities values are depicts in Fig. 7. The biggest values meet in the neighborhoods of the walls, mainly near the downstream wall; regions that coincide with the zones of high gradients of speed of the primary eddy. In function that the Smagorinsky sub-grid model it supplies high values of turbulent viscosity in the parietal regions, the statistics of the fluctuating velocity one does not behave adequately in the regions near the walls and, probably this is the reason not to obtain a good agreement with the experimental data in other regions of the cavity. Is possible to differentiate the advantage of a value of C_s =0.18, mainly seeing the $u\ rms$ velocity. Again the dynamic sub-grid scale model obtain better agreement with experimental data in all regions.

The difference between the results simulated with the experimental data registered in Figs. 6 and 7, in peak magnitude, is probably due to necessity to use of denser meshes.

The Taylor-Gortler-like vortices are originated due the hydrodynamics instability near of upstream wall (Chiang and Sheu 1997) and the development of these counter-rotating vortices were observed for Re =1000 by Prasad and Koseff

(1984), but recently Migeon et al. (2003) show that no well-formed counter-rotating vortices emerge for Re =1000, only initial phase of the instability development are revealed. For Re =3200 The Taylor-Gortler-like vortices are lightly unstable, but for Re =10000 this complex structures are highly unstable and distorted, as observed in Fig. 8. Moreover these structures are coupled with the primary and secondary eddies. The instantaneous vorticity (xy) isosurfaces at Re =10000 are plotted in Fig. 8, for the Smagorinsky sub-grid model with C_s =0.18 (left) and for dynamic sub-grid scale model (right). The three-dimensional flow structures with dynamic model present a strongly quantity and quality of details.

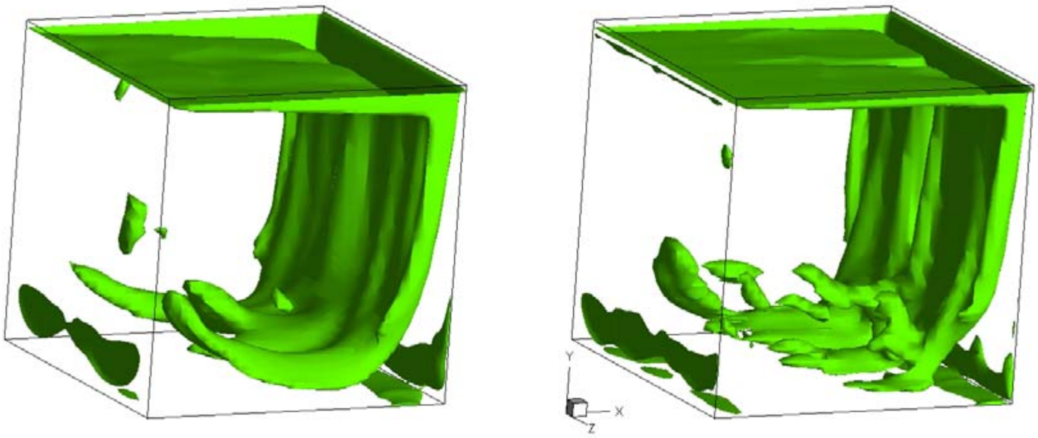

Figure 8. Instantaneous vorticity isosurfaces at Re =10000. Left: Smagorinsky model; right: dynamic model.

5. Conclusions

Solving the Navier-Stokes equations has performed stable and unstable flows in a three-dimensional lid-driven cavity. The large-eddy simulation with Smagorinsky and dynamic sub-grid scale models was used for flows of $Re \geq$ 3200. The pattern of stable flows of bi and three-dimensional configurations were reproduced with good agreement respect of results of other authors. Characteristic Three-dimensional flow structures, as the end-wall corner vortices, the spanwise inward and outward currents and the Taylor-Gortler-like, appear as Reynolds number increased and becomes highly unstable for high Reynolds number. Quantitative comparisons between the Smagorinsky and dynamic sub-grid scale model and experimental dates, for turbulent flow, shown advantage of dynamic model; moreover the qualitative results were widely superiors.

6. Acknowledgements

The authors would like to tank FAPEMIG and CENPES/PETROBRAS for the financial support.

7. References

Babu, V. and Korpela, S.A., 1994, “Numerical Solution of the Incompressible three-dimensional Navier-Stokes Equations”, Computers Fluids 23(5). Pp. 675-691.

Benjamin, A.S. and Denny V.E., 1979, “On the Convergence of Numerical Solutions for 2D Flows in a Cavity Large Re”, J. Comput. Phys. 33, pp. 340-358.

Botella, O., and Peyret, R., 1998, “Benchmark Spectral Results on the Lid-Driven”, Comput Fluids, vol 27(4), pp. 421-433.

Deshpande, M.D. and Milton, S.G., 1998, “Kolmogorov Scales in a Driven Cavity Flow”, Fluid Dyn. Res. 22, pp. 359-381.

Ghia, U., Ghia, K.N. and Shin, C.T., , “High-Re Solutions for Incompressible Flow Using the Navier-Stokes equations and a Multigrid Method”, J. Comput. Phys. 48, pp. 387-411.

Goyon, O. 1996, “High-Reynolds number solutions of Navier-Stokes Equations Using Incremental Unknowns” Comp. Methods in Applied Mech. and Eng. 130, pp. 319-335.

Gravemeier, V., 2003, 1982, “The Variational Method for Laminar and Turbulent Incompressible Flow”, Doctor Thesis, Universität Stuttgart.

Hassan, Y.A. and Barsamian, H.R., 2001, “New-wall Modeling for Complex Flows Using the Large Eddy Simulation Technique in Curvilinear Coordinates”, Int. J. Heat and Mass Transfer, 44, pp. 4009-4026.

Iwatsu, R. Ishi, K., Kawamura, T., Kawahara, K. and Hyun, J.M., 1989, “Simulation of Transition to Turbulence inm a Cubic Cavity”, AIAA Pap. No 98-0040.

Iwatsu, Hyun, J.M., and Kawahara, K., 1990, “Analyses of Three-dimensional Flow Calculations in a Driven Cavity”, Fluid Dyn. Res., 6, pp. 91-102.

Kato, Y., Kawai, H., and Tanahashi, T., “Numerical Flow Analysis in a Cubic Cavity by the GSMAC finite-element method”, JSME Int. J. Series II 33, pp.649-658.

Koseff, J.R. and Street R.L., 1984, “Visualization of a Shear driven three-dimensional recirculation flow”, J. Fluids Eng. 106, pp. 21-29.

Ku, H.C., Hirsh, R.S. and Taylor, T.D., 1987, “A Pseudospectral Method for Solutions of the Three-dimensional Incompressible Navier-Stokes Equations”, J. Comput. Phys. 70, pp. 439-462.

Migeon, C., Pineau, G. and Texier, A., 2003, “Three-dimensionality development inside standard parallelepipedic lid-driven cavities at Re=1000”, J. of Fluids and Structures Eng. 17, pp. 717-738.

Padilla, E.L.M., 2004, “Large-Eddy Simulation of Transition to Turbulence in Rotating System with Heat Transfer”, Doctor Thesis, Universidade Federal de Uberlândia.

Padilla, E.L.M. and Silveira-Neto, A., 2003, “Influence of Different Types of Filters for Dynamic Modeling in Large-Eddy Simulation”, Proceedings of XXIV Iberian Latin-American Congress on Computational Methods in Engineering, Ouro Preto-MG, pp. CIL189-32.

Patankar, S.V., 1980, “Numerical Heat transfer and Fluid Flow”, Hemisphere Publishing Corporation, New York.

Schreiber, R. and Keller H.B., 1983, “Driven Cavity Flows by Efficient Numerical Techniques”, J. of Comp. Physics, 49, pp. 310-333.

Sheu, T.W.H. and Tsai, S.F., 2002, “Flow Topology in a Steady Three-Dimensional Lid-Driven Cavity”, Comput Fluids 31, pp. 911-934.

Zang, Y., Street, R.L. and Koseff, J.R., 1994, “A Non-Staggered Grid, Fractional Step Method for Time-Dependent Incompressible Navier-Stokes Equations in Curvilinear Coordinates”, J. Comp. Phys. 114, pp. 18-33.

5. Responsibility notice

The authors are the only responsible for the printed material included in this paper.